RASĀYAN *J. Chem.*
Vol. 19 | No. 3 | 1607-1614 | July-September | 2026
ISSN: 0974-1496 | e-ISSN: 0976-0083 | CODEN: RJCABP
http://www.rasayanjournal.com
http://www.rasayanjournal.co.in

DFT INSIGHTS INTO THE EFFECT OF SUBSTITUENTS ON THE REARRANGEMENT OF SILYLOXYACETYLENES TO SILYLKETENES

J. Tyagi and S. K. Mishra✉
Department of Chemistry, Zakir Husain Delhi College, University of Delhi, Delhi-110002
✉Corresponding author: drsanjeevkmishra@zh.du.ac.in

ABSTRACT

The current study investigates the rearrangement reaction mechanism of silylketenes from Silyloxyethyne, 1-Silyloxypropyne and 2-Silylsilyloxyethyne via three paths (Path 1, 2, and 3) using DFT calculations. All the three rearrangement reactions are exothermic, with Path 2 being the least exothermic. A planar four-membered transition structure with a single imaginary frequency (~ 400) is obtained for all the three paths. Only minor variations in ΔE values are observed among the three pathways. Also, the introduction of methyl and silyl groups has no significant effect on the activation energy of the three reaction paths. The formation of C-Si and dissociation of the O-Si bond are indicated by structural parameters, charge density, Laplacian density, and natural atomic charge values. Our results indicate that DFT calculations provide reliable results at a low computational cost. Theoretical study of these reactions is important, as the product silylketene undergoes side reactions with the reactant itself, making experimental determination of reaction enthalpy challenging. This work provides insight into the reaction mechanisms, the effect of substituents (methyl and silyl groups), and contributes to the advancement of quality education.

Keywords: B3LYP, NBO Analysis, Mechanism, 1,3-silyl Shift, Intrinsic Reaction Coordinate (IRC), Silylynol Ethers.

INTRODUCTION

Experimental and computational studies are used to understand the reaction mechanisms for the different types of reactions, viz., rearrangement, substitution, elimination, etc. However, when experimental investigations are not viable, computational studies provide valuable insights for elucidating reaction pathways.[1] The present work illustrates this approach, as $H_3SiC(H)=C=O$, the smallest silylketene, is intrinsically unstable and displays a distinct tendency toward self-reaction. Computational studies provide a suitable way to examine and rationalise the underlying reaction mechanisms of such reactive molecules. Silyl ynol ethers with the general formula, $R_3Si\text{-}O\text{-}C{\equiv}C\text{-}R$, are organosilicon compounds that find their uses in many organic synthesis reactions. These compounds, owing to their stability, ambident reactivity, and bonding, possess high synthetic value. Silyl enol ethers are used as precursors to ketenes and silylketenes. Photolysis or heating of silyl ynol ethers yields silylketenes via a rearrangement reaction. Substituted silylketenes can also be synthesised from other reagents such as ethoxy(trimethylsilyl)acetylene.[2] Silylketenes, having the general formula, $R_3SiC(H)=C=O$, are also a class of organosilicon compounds in which a ketene functional group is bonded to a silyl substituent. The silyl group imparts both steric protection as well as electronic stabilisation via the hyperconjugation effect to the otherwise thermally unstable and reactive ketenes. Similar to the ketenes, these compounds are also reactive towards nucleophiles and undergo cycloaddition reactions. Silylketenes are highly valuable and versatile reagents in organic synthesis. They play a vital role in various transformation reactions, e.g., the Wittig reaction, insertion reaction of diazomethane, Lewis acid-catalysed [2+2] cycloadditions with carbonyl compounds, nucleophilic addition reaction of carbon or heteroatoms, etc.[3,4] The smallest silylketene, $H_3SiC(H)=C=O$, is thermodynamically difficult to synthesize. Also, the kinetic instability of this organic compound towards oxygen and water further makes the synthesis process more challenging and complicated using traditional preparative synthesis chemistry. However, in the year 2017, Tarczay *et al.* successfully reported its gas-phase synthesis at low temperature from the interaction of highly

http://doi.org/10.31788/RJC.2026.1939772

energetic electrons and ices made of silane and carbon monoxide.[5] *Ab initio* calculations were also performed to confirm the silylketene formation and to investigate its formation mechanism. Various studies, experimental as well as theoretical (semi-empirical and ab-initio) have reported the synthesis, applications and reaction mechanisms of silylketenes.[6-10] The present DFT work investigates the silyloxyacetylenes rearrangement to silylketenes in the vacuum phase to gain more insight into their reaction mechanisms via 1,3-silyl shift. Three paths are studied in detail for silyloxyethyne, 1-silyloxypropyne, and 1-silyloxysilylethyne rearrangement to the corresponding silylketene. The effect of methyl and silyl group substitution is also investigated. This theoretical work helps improve the understanding of silylketenes formation mechanism from silyloxyacetylenes and contributes to achieving one of the goals of SDGs, i.e., quality education (SDG-4).

EXPERIMENTAL

Method of Calculation

Three reaction paths (Path 1, 2, and 3), considered in the current study, were explored using density functional theory (DFT) via B3LYP/6-311++G(d,p) method. The GAUSSIAN-09 software package was used for carrying out all the calculations. Geometry optimisation, along with the frequency calculation, was carried out to explore the geometries and perform the thermochemical calculations for reactants, transition states, and products.[11-13] To investigate the bond properties, electronic charge density (ρ_c) and Laplacian density ($\nabla^2\rho_c$) were calculated using the AIM command.[14] Natural charges present on the atoms in the reactant, product and transition state for all three paths were investigated using NBO analysis. Changes in ρ_c and $\nabla^2\rho_c$ values, along with natural atomic charges, help to look into the mechanistic aspect of the reaction for all the paths. Harmonic vibrational frequency calculations established the stationary states for the reaction paths.[15] Intrinsic Reaction Coordinate (IRC) calculation and its plots were studied for the transition state of the three paths. E_a (activation energy) and ΔE (energy of reaction) were also calculated and compared with the results of HF and MP2 calculations using the same basis set.[16-19]

RESULTS AND DISCUSSION

Silyloxyethyne, 1-Silyloxypropyne and 2-Silylsilyloxyethyne rearrange to corresponding silylketene via Path 1, Path 2, and Path 3, respectively. Figure-1 depicts the general outline for the reaction paths. The geometries of the reactant, transition state (TS) and the corresponding product after the rearrangement are shown in Fig.-2. The optimised geometrical parameters, calculated using B3LYP/6-311++G(d,p) method, are listed in Table-1.

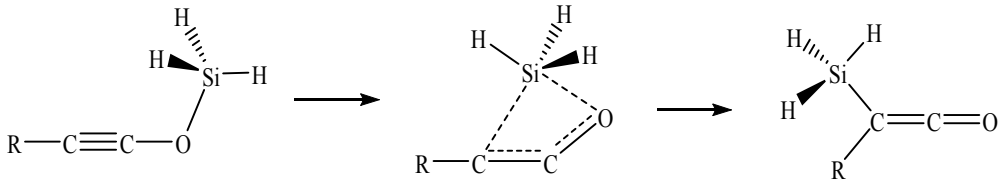

Path 1: R=H; Path 2: R=CH_3; Path 3: R=SiH_3

Fig.-1: Rearrangement Reaction of Silyloxyalkyne to Corresponding Silylketene

Path 1: Silyloxyethyne Rearrangement to Silylketene

Path 1 shows the conversion of Silyloxyethyne (‘1’) to the corresponding silylketene (‘2’) via a 1,3-silyl shift in Fig.-2. This rearrangement reaction takes place through the transition state, ‘TS12’. There is a significant decrease in the C2-O1-Si5 bond angle from 124.8° to 73.7°. Also, we can see the slight bending of the bond angle C3-C2-O1 from almost straight, i.e., 178.6°, to 166.8° in ‘TS12’. This decrease in the bond angle helps in the formation of TS. Furthermore, in the ‘TS12’, the O1-Si5-C3 and Si5-C3-C2 bond angles were observed to be 64.4° and 55.1°, respectively. The magnitude of the dihedral angle, C3-C2-O1-Si5 and C2-O1-Si5-H7 in the ‘TS12’ suggests that the TS is a planar four-membered structure. As the ‘TS12’ formation takes place, the O1-Si5 bond elongates from 1.703 Å in reactant (‘1’) to 2.047 Å in ‘TS12’. This observation is further supported by a decrease in $\rho(r_c)$ value (Table-2) in AIM calculations.

A decrease in $\nabla^2\rho_c$ value from 0.694 to 0.106 for this bond in 'TS12', as compared to reactant ('1'), shows a decrease in the ionic character, indicating the ongoing 1,3-silyl shift. This O1-Si5 bond breaks in the product '2' since no value for the $\rho(r_c)$ and $\nabla^2\rho_c$ is obtained. Some interaction between C3 and Si5 was observed in the 'TS12' as the distance between the two is 2.525 Å. The $\rho(r_c)$ and $\nabla^2\rho_c$ value for the C3-Si5 bond in product '2', as compared to no value in reactant '1', indicates the formation of the new bond. Also, the C3-Si5 bond length in '2' was observed to be 1.863 Å. Natural atomic charges were calculated using NBO analysis (Table-3). Silyl shift is accompanied by a decrease of negative charge on O1 and an increase of negative charge on C3, synchronised with a slight decrease in positive charge on Si5. These changes in the charge values on O1 and C3 also support the shift of Si5 (electropositive atom) from O1 to C3. Furthermore, the C2 atom becomes more electropositive in product '2' (0.719) as compared to reactant '1' (0.309), since it is attached to C3 and O1 via a double bond on the both the sides in the product '2'. The frequency analysis with intensities of the reactant, TS, and product confirms the nature of species, e.g., a positive value for reactant '1' and product '2' indicates the stable geometries for the two. The single imaginary vibrational frequency for the 'TS12' (Table-4) confirms the valid TS structure. Also, the IRC path (Fig.-3) further validates the obtained TS.

Path 2: 1-Silyloxypropyne Rearrangement to Silyl(methyl)ketene

Path 2 studies 1-silyloxypropyne ('3') rearrangement to corresponding silyl(methyl)ketene ('4') as represented in Fig.-2. As in the Path 1, the TS for this path, 'TS34', is also signified by a substantial decrease in C2-O1-Si5 bond angle from 124.0° to 71.6° and an increase in O1-Si5 bond length from 1.697 Å to 2.046 Å. The $\nabla^2\rho_c$ values of the C2-O1 bond change from a negative value in '3' to a positive value in '4', indicating the change in nature of bonding, i.e., covalent to ionic. Furthermore, ρ (r_c) and $\nabla^2\rho_c$ values for the C3-Si5 bond in the product '4' confirm the formation of a new bond. The changes observed in the bond angle O1-Si5-C3 and Si5-C3-C2 are similar to those in the Path 1. The bond angle, C4-C3-C2, magnitude changes to 121.7° (in '4') from 180° (in '3') to accommodate the shifted silyl group on the C3 atom and reduce the steric hindrance. Similar to 'TS12', the 'TS34' also possess a planar structure as suggested by the magnitude of dihedral angles, C3-C2-O1-Si5 and C2-O1-Si5-H7. The natural atomic charges on the various atoms in Path 2 are similar to those in Path 1, except for the less negative charge on the C3 atom in '3' and '4' by 0.244 and 0.221, respectively. This change in charge on C3 is due to the replacement of an H atom by a methyl group on the C3 atom. The data of charge distribution indicates that the methyl group is inductively electron-withdrawing in nature as compared to the H atom. This observation is in concordance with the recently published computational study by Elliott et al. in the year 2025 on the nature of alkyl groups in organic compounds.[20] Vibrational frequency analysis data with intensities of '3', 'TS34' and '4' (Table-4) suggest the stable geometries of the reactant and product. Also, only one negative frequency for the TS indicates an acceptable TS structure. The IRC plot for the Path 2, shown in Figure-3, further supports the valid and acceptable TS geometry.

Path 3: 2-Silylsilyloxyethyne Rearrangement to Disilylketene

Path 3, shown in Fig.-2 depicts how 2-Silylsilyloxyethyne ('5') rearranges to disilylketene ('6') via 'TS56'. The structural changes with respect to bond length, bond angle, and dihedral angle observed in Path 3 are similar to those in Path 1 and Path 2. During the rearrangement of '5' to '6', the Si4-C3-C2 bond angle changes to 118.5° from linear (179.5°). This change in bond angle is observed to reduce the steric hindrance due to the 1,3-silyl shift on the C3 atom from O1. The structure of 'TS56' is also planar in this path. Changes in the magnitude of ρ (r_c) and $\nabla^2\rho_c$ for the various bonds during the transition of '5' to '6' are also similar to the two other paths discussed above. The charges obtained from the NBO analysis on the different atoms are found to be consistent with the path 1 and path 2. However, the charges observed on the C3 atom are different. The charge on the C3 atom in '5' is most negative (-0.617) as compared to the two other reactants, i.e., '1' and '3'. This is due to the silyl group attached to the C3 atom in '5' as compared to H in'1' and the methyl group in '3'. These observations are consistent with the electropositive nature of Si. During the rearrangement, charges in 'TS56' increase to a more negative value on C3 owing to the fact of silyl group shifts to the C3 atom. Furthermore, the most negative charge of magnitude 1.199 on C3 in '6' established the electron-donating nature of the Si atom. The vibrational

frequency analysis, along with intensities (Table-4), indicates the stable geometries of reactant '5' and product '6' with all positive values. The single imaginary frequency obtained for 'TS56' (370*i*) also establishes the valid TS geometry. The IRC plot for this rearrangement is shown in Fig.-3.

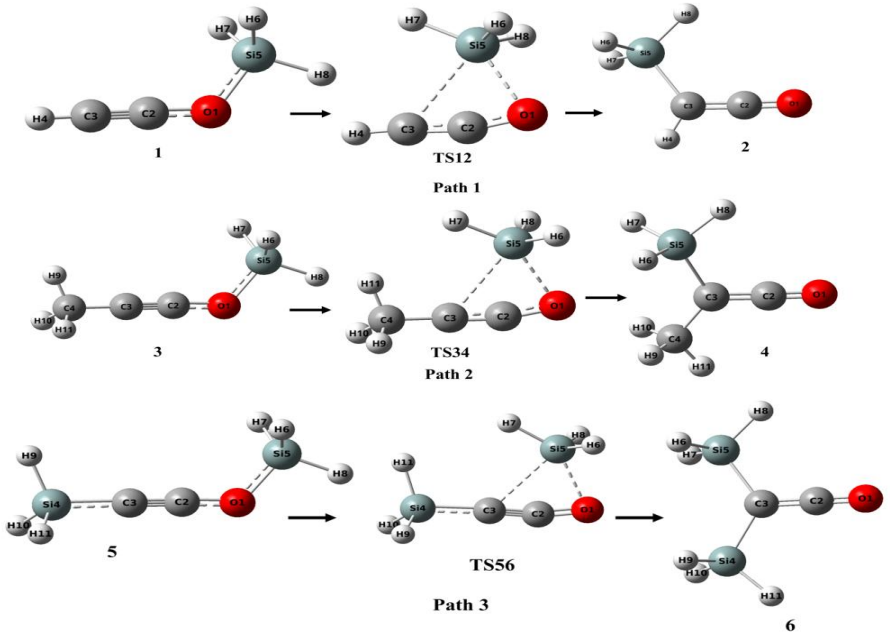

Fig.-2: Optimised Geometry of Products, Reactants and TSs for Path 1, 2, and 3

Table-1: Selected Geometric Parameters using B3LYP/6-311++G(d,p)

	Path 1			Path 2			Path 3		
System[b]	1	TS12	2	3	TS34	4	5	TS56	6
Bond Lengths (in Å)									
C2-C3	1.201	1.225	1.310	1.202	1.227	1.309	1.212	1.225	1.306
O1-C2	1.296	1.261	1.161	1.306	1.271	1.165	1.291	1.261	1.162
O1-Si5	1.703	2.047	-	1.697	2.046	-	1.707	2.047	-
H4-C3	1.060	1.062	1.085	-	-	-	-	-	-
Si5-C3	-	2.525	1.863	-	2.492	1.868	-	2.525	1.871
C4-C3	-	-	-	1.460	1.458	1.527	-	-	-
Si4-C3	-	-	-	-	-	-	1.815	1.819	1.871
Bond Angles (in Degrees)									
C3-C2-O1	178.6	166.8	178.3	177.9	168.5	178.7	178.3	168.8	180.0
C2-O1-Si5	124.8	73.7	-	124.0	71.6	-	125.6	73.7	-
O1-Si5-C3	-	64.4	-	-	65.5	-	-	63.8	-
Si5-C3-C2	-	55.1	122.1	-	54.3	117.0	-	53.7	118.5
C4-C3-C2	-	-	-	179.9	179.8	121.7	179.5*	177.4*	118.5*
C3-Si5-H7	-	82.2	110.5	-	81.0	110.0	-	81.7	109.9
Dihedral Angles (in Degrees)									
C3-C2-O1-Si5	-179.9	0.1	-0.2	179.9	0.0	0.0	-179.9	0.0	-179.9
C2-O1-Si5-H7	-60.4	-0.1	-	-60.3	0.0	-	-60.3	0.0	-
H4-C3-C2-O1	-0.4	-179.8	179.8	-	-	-			
C4-C3-C2-O1	-	-	-	5.9	171.1	-179.9	-	-	-
Si4-C3-C2-O1	-	-	-	-	-	-	5.2	-179.2	161.9

[a]See Fig.-2, *Si4-C3-C2

Table-2: Some Selected Bonding Characteristics of Reaction Paths using B3LYP/6-311++G(d,p) Optimized Geometry

Path 1						
System[a]	1		TS12		2	
	$\rho(r_c)$	$\nabla^2\rho_c$	$\rho(r_c)$	$\nabla^2\rho_c$	$\rho(r_c)$	$\nabla^2\rho_c$
C2-O1	0.322	-0.259	0.368	-0.543	0.455	0.178
C3-C2	0.392	-0.932	0.378	-0.901	0.326	-0.678
O1- Si5	0.114	0.694	0.060	0.106	-	-
C3-Si5	-	-	-	-	1.642	0.249
Path 2						
System[a]	3		TS34		4	
	$\rho(r_c)$	$\nabla^2\rho_c$	$\rho(r_c)$	$\nabla^2\rho_c$	$\rho(r_c)$	$\nabla^2\rho_c$
C2-O1	0.323	-0.252	0.360	-0.576	0.450	0.157
C3-C2	0.389	-0.923	0.376	-0.926	0.328	-0.705
O1- Si5	0.113	0.689	-	-	-	-
C3-Si5	-	-	-	-	0.114	0.239
C2-Si5	-	-	0.066	0.114	-	-
Path 3						
System[a]	5		TS56		6	
	$\rho(r_c)$	$\nabla^2\rho_c$	$\rho(r_c)$	$\nabla^2\rho_c$	$\rho(r_c)$	$\nabla^2\rho_c$
C2-O1	0.326	-0.242	0.371	-0.503	0.454	0.156
C3-C2	0.384	-0.839	0.369	-0.828	0.326	-0.651
O1- Si5	0.112	0.681	-	-	-	-
C3-Si5	-	-	-	-	0.110	0.230
C2-Si5	-	-	0.060	0.098	-	-

[a]See Fig.-2, ρ_c in e/au^3 and $\nabla^2\rho_c$ in e/au^5

Table-3: Natural Atomic Charges

	Path 1			Path 2			Path 3		
System[a]	1	TS12	2	3	TS34	4	5	TS34	6
O1	-0.796	-0.671	-0.443	-0.798	-0.674	-0.452	-0.783	-0.648	-0.449
C2	0.309	0.241	0.719	0.285	0.193	0.705	0.373	0.265	0.726
C3	-0.379	-0.421	-0.976	-0.135	-0.147	-0.755	-0.617	-0.659	-1.199
H4	0.228	0.253	0.281	-0.635*	-0.633*	-0.556*	0.870**	0.885**	0.934**
Si5	1.188	1.113	0.906	1.191	1.110	0.916	1.182	1.120	0.934

[a]See Fig.-2
*C4 & **Si4

Table-4: Calculated Harmonic Vibrational Frequencies (cm^{-1}) using B3LYP/6-311G++ (d, p) Optimised Geometry

1		TS12		2	
553 (68)	1137 (245)	389i	996 (60)	412 (31)	1275 (39)
587 (82)	2176 (144)	317 (87)	1157 (105)	595 (23)	2129 (973)
657 (58)	2189 (118)	331 (72)	2078 (211)	672 (86)	2152 (126)
677 (40)	2201 (250)	590 (95)	2116 (174)	776 (49)	2171 (182)
718 (41)	2220 (65)	683 (44)	2187 (52)	915 (51)	
921 (79)	3382 (120)	699 (44)	2218 (97)	916 (276)	
926 (268)		850 (119)	3367 (132)	946 (116)	
941 (166)		980 (227)		1045 (30)	
3		TS34		4	
678 (44)	2174 (71)	344i	992 (61)	624 (28)	2141 (126)
717 (53)	2181 (126)	308 (72)	1286 (158)	647 (51)	2170 (156)
842 (178)	2213 (112)	552 (113)	2067 (161)	909 (83)	2925 (40)
921 (78)	2321 (204)	682 (42)	2186 (85)	910 (278)	
928 (233)	2922 (45)	759 (21)	2194 (185)	943 (101)	
944 (171)		854 (143)	2215 (102)	1076 (20)	
1265 (262)		980 (204)		2113 (1017)	

5		TS56		6	
499 (26)	1239 (152)	370i	932 (103)	582 (28)	2157 (222)
667 (72)	2154 (120)	319 (88)	975 (189)	669 (28)	2169 (98)
669 (52)	2155 (121)	494 (179)	990 (58)	685 (93)	2173 (214)
676 (30)	2157 (235)	563 (30)	1268 (45)	892 (626)	
703 (207)	2181 (97)	628 (24)	2098 (528)	913 (20)	
719 (153)	2194 (111)	657 (48)	2123 (189)	915 (102)	
909 (741)	2222 (206)	673 (54)	2157 (71)	927 (59)	
921 (61)	2233 (444)	679 (39)	2165 (104)	949 (234)	
927 (70)		852 (191)	2167 (71)	1290 (34)	
929 (54)		908 (297)	2191 (53)	2116 (1118)	
944 (112)		919 (53)	2221 (91)	2153 (61)	

[a]See Fig.-2 [b]Scaled by 0.9679
[c]Values in the parentheses are intensities in km/mol

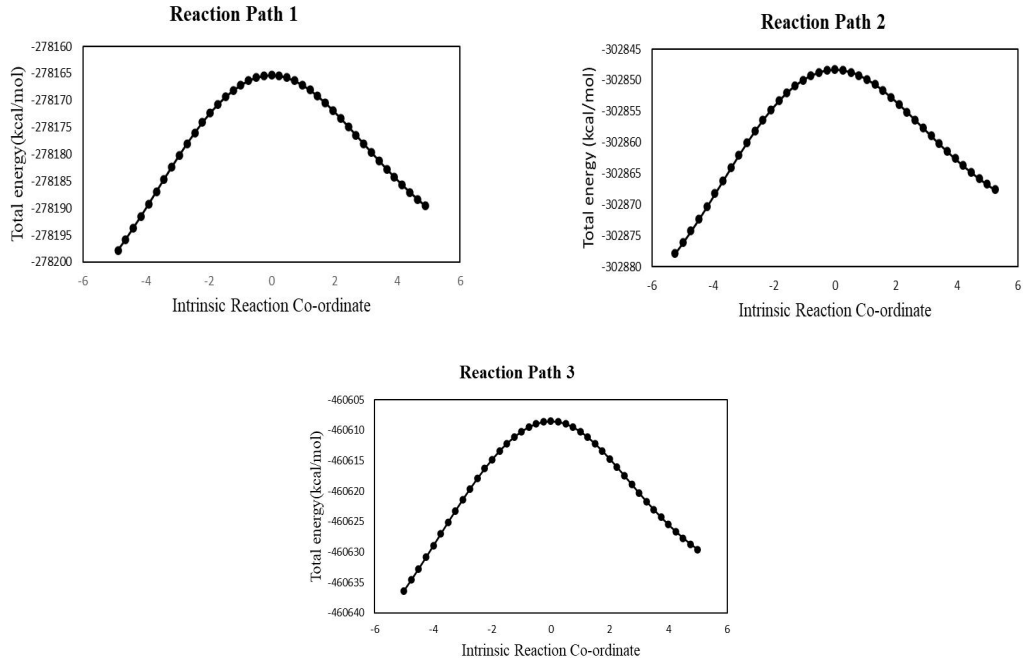

Fig.-3: Potential Energy Profile (PES) for Reaction Path 1, Path 2, and Path 3. Zero Point on the x-axis represents the Transition State Along the IRC with Negative Values Towards the Reactant and Positive Values Towards the Product. B3LYP/6-311G++(d,p) was used for all These Calculations

Energetics of the Three Reaction Paths (1, 2, and 3)

The E_a and ΔE of the rearrangement reaction for the three considered paths, viz., Path 1, 2, and 3, are tabulated in Table-5. For all the energetic calculations, the 6-311++G(d,p) basis set is used at HF, MP2 and B3LYP levels of calculation to do the comparison between *ab initio* and DFT. The silylketenes are stable as compared to normal ketenes because of the silyl group. However, they are still kinetically reactive and are handled under inert and anhydrous conditions. The silylketene product formed experimentally readily undergoes reaction with the remaining reactants and can undergo a side reaction such as [2+2] cycloaddition. Thus, experimental determination of the reaction enthalpy is difficult and therefore has not been obtained. The low ΔE values obtained in our study for the different paths further support the fact. All the three reactions are found to be exothermic in nature. The magnitude of ΔE for Path 2 is the least among the three considered paths. The order of ΔE for the different paths is observed to be Path 2 < Path 3 < Path 1. The values obtained for E_a and ΔE at the MP2 and DFT level of calculation are close to each other as compared to values at the HF level of calculation for all three paths. The E_a

values for Path 1 are only slightly higher compared to the other two paths (2 and 3) at all three levels of calculations, suggesting that the effect of the methyl and silyl group is not much on the energetics of the reaction. This observation also supports the fact of the high reactivity of silylketenes.

Table-5: Calculated Activation Energies (E_a) and Energy of Reaction (ΔE) (in kcal mol^{-1})

Reaction[a]		A	B	C
Path 1	E_a	49.0	36.5	36.7
	ΔE	-21.4	-23.6	-24.6
Path 2	E_a	47.9	34.5	35.3
	ΔE	-14.2	-19.0	-17.9
Path 3	E_a	47.6	34.4	35.5
	ΔE	-17.8	-22.2	-21.0

[a]See Fig.-2
A. HF/6-311++G(d,p) optimized geometry
B. MP2/6-311++G(d,p) optimized geometry
C. B3LYP/6-311++G(d,p) optimized geometry

CONCLUSION

The current study discussed the formation mechanism of the silylketenes from Silyloxyethyne, 1-Silyloxypropyne and 2-Silylsilyloxyethyne via three paths (Path 1, 2, and 3). All the three rearrangement reactions are observed to be exothermic. Among all three paths, Path 2 is the least exothermic at all levels of calculations. The rearrangement reaction proceeds through a planar four-membered transition structure. In all the three reactions, an acceptable transition state structure is obtained with a single negative frequency of magnitude near 400. All the reactants and products considered in the study possess stable geometry, as reflected in the all-positive values of vibrational frequencies. The energetic data suggest that the variation in ΔE values is very close in all the three paths. Furthermore, the E_a data also indicate that the effect of the methyl and silyl groups is not significant on the activation energy. The formation of a new bond between C and Si and the dissociation of the O-Si bond are supported by the structural parameters, electronic charge density (ρ_c), Laplacian density ($\nabla^2\rho_c$), and natural atomic charge values. A comparison of the MP2 and DFT methods indicates that DFT calculations, which include both exchange and correlation effects, provide reliable results while maintaining a low computational cost. Theoretical investigation of these rearrangement reaction pathways is particularly important, as the product silylketene readily undergoes side reactions with the reactant itself, making experimental determination of E_a and ΔE challenging. This study provides insight into the reaction mechanisms and contributes to the advancement of quality education, aligning with the objectives of SDG-4.

ACKNOWLEDGEMENTS

Both authors are grateful to Zakir Husain Delhi College and the University of Delhi for providing the necessary resources for the present work.

CONFLICT OF INTEREST

The authors declare that there is no conflict of interest.

AUTHOR CONTRIBUTIONS

The present work is contributing to *SDG-4: Quality Education*. Both the authors have contributed significantly to this manuscript, participated in reviewing/editing and approved the final draft for publication. The research profile of the authors can be verified from their ORCID ids, given below:

Sanjeev Kumar Mishra https://orcid.org/0009-0006-1555-3128
Jyoti Tyagi https://orcid.org/0000-0002-2689-8440

Cite this article as: J. Tyagi and S. K. Mishra, *Rasayan J. Chem.*, 19(3), 1607-1614(2026), https://doi.org/10.31788/RJC.2026.1939772

REFERENCES

1. J. Tyagi, R. Mishra and S. K. Mishra, *Rasayan Journal of Chemistry*, **18(4)**, 1927(2025), http://doi.org/10.31788/RJC.2025.1849395
2. L. L. Shchukovskaya, R. I. Pal'chilk and A. N. Lazarev, *Doklady Akademii Nauk SSSR,* **164(2)**, 357(1965), https://www.mathnet.ru/eng/dan31584
3. A. Pommier, Kocienski and J. M. Pons, *Journal of the Chemical Society, Perkin Transactions,* **1, Issue 13**, 2105(1998), https://doi.org/10.1039/A801254G
4. R. L. Danheiser, Chapter-2 in Science of Synthesis 23, Category 3, Compounds with Four and Three Carbon Heteroatom Bonds, 2006, 1st Edition, Georg Thieme Verlag KG, Stuttgart. http://www.thieme-connect.de/products/ebooks/book/10.1055/b-003-121810
5. G. Tarczay, M. Förstel, S. Góbi, P. Maksyutenko and R. I. Kaiser, *ChemPhysChem,* **18(8)**, 882 (2017), https://doi.org/10.1002/cphc.201601422
6. H. Sakurai, A. Shirahata, K. Sasaki and A. Hosomi, *Synthesis,* **1979(9)**, 740(1979), https://doi.org/10.1055/s-1979-28823
7. A. Moyano, M. A. Pericas, F. Serratosa and E. Valenti, *Journal of Organic Chemistry,* **52(25)**, 5532(1987), https://doi.org/10.1021/jo00234a007
8. M. Oblin, M. Rajzmann and J. M. Pons, *Tetrahedron,* **53(24)**, 8165(1997), https://doi.org/10.1016/S0040-4020(97)00503-6
9. M. Oblin, F. Fotiadu, M. Rajzmann and J. M. Pons, *Journal of the Chemical Society, Perkin Transactions,* **2(9)**, 1621(1997), https://doi.org/10.1039/A703439C
10. A. D. Allen and T. T. Tidwell, *Tetrahedron Letters,* **32(7)**, 847(1991), https://doi.org/10.1016/S0040-4039(00)92101-4
11. A. D. Becke, *Physical Review A,* **38**, 3098(1998), https://link.aps.org/doi/10.1103/PhysRevA.38.3098
12. A. D. Becke, *Journal of Chemical Physics,* **98(7)**, 5648(1993), https://doi.org/10.1063/1.464913
13. C. Lee, W. Yang and R. G. Parr, *Physical Review B,* **37**, 785(1998), https://doi.org/10.1103/PhysRevB.37.785
14. R. F. W. Bader, *Accounts of Chemical Research,* **18(1)**, 9(1985),https://doi.org/10.1021/ar00109a003
15. M. P. Andersson and P. Uvdal, *Journal of Physical Chemistry A,* **109(12)**, 2937(2005), https://doi.org/10.1021/jp045733a,
16. W. J. Hehre, L. Radom, P. R. Schleyer and J. A. Pople, *Ab-initio Molecular Orbital Theory,* pp. 548(1986), https://doi.org/10.1002/jcc.540070314
17. R. G. Parr and W. Yang, *Density Functional theory of Atoms and Molecules,* pp.IX+333(1989), https://doi.org/10.1002/qua.560470107
18. J. K. Labanoeski and J. W. Andzelin, *Density Functional Methods in Chemistry,* Springer(1991), https://doi.org/10.1007/978-1-4612-3136-3
19. S. H. Vosko, L. Wilk and M. Nusair, *Canadian Journal of Physics,* **58(8)**, 1200(1980), https://doi.org/10.1139/p80-159
20. M. C. Elliott, C. E. Hughes, P. J. Knowles and B. D. Ward, *Organic and Biomoecular Chemistry,* **23**, 352(2025), https://doi.org/10.1039/D4OB01572J

[RJC-9772/2026]